UNCECOMP 2015
1st ECCOMAS Thematic Conference on
Uncertainty Quantification in Computational Sciences and Engineering
M. Papadrakakis, V. Papadopoulos, G. Stefanou (eds.)
Crete Island, Greece, 25–27 May 2015

POSTERIOR ROBUST OPTIMIZATION FOR DESIGN UPDATE BASED ON MEASUREMENTS

Dimitrios I. Papadimitriou, and Costas Papadimitriou

Department of Mechanical Engineering, University of Thessaly
Pedion Areos, 38334, Volos, Greece
e-mail: dpapadim@uth.gr, costasp@uth.gr

Keywords: Optimal Sensor Location, Uncertainty Quantification, Uncertainty Propagation, Robust Optimization

Abstract. *A Bayesian unified framework is proposed for data-informed robust design optimization. Models of uncertainties postulated in conventional robust design optimization are treated as prior uncertainties in a Bayesian context. Measurements collected for one or more components of the system to be designed are used by standard Bayesian inference tools to update uncertainties at component level and quantify these uncertainties by posterior PDFs. For the data-informed model parameters, approximations of uncertainty models by Gaussian posterior PDFs, arising from the use of Bayesian central limit theorem, are particularly suited for certain methods used for robust design optimization, such as first-order or Taylor expansion techniques or sparse grid methods required to estimate the multi-dimensional integrals that arise in the robust objective functions. The posterior robust design optimization framework is demonstrated by applying it to the optimization of the aerodynamic shape of an airfoil under data-informed turbulence model uncertainties estimated from measurements on simplified flows such as flow over a flat plate, and prior uncertainties postulated for the Mach and angle of attack.*

1 INTRODUCTION

The Bayesian inference framework for quantifying and propagating uncertainties in computational models of engineering systems has been adequately developed and widely used. The framework aims at the selection among alternative plausible model structures to represent physical phenomenon and the unmodelled dynamics, estimation of the uncertainties in the parameters of these model structures, as well as propagation of uncertainties through the model to make robust predictions of output quantities of interest (QoI), consistent with available experimental measurements. Herein, the use of the Bayesian framework for posterior robust design optimization given measurement data at system components level is addressed.

The four steps involved in the posterior robust design optimization are presented. The first step is the optimization of the locations of the sensors [1, 2, 3, 4, 5, 6] so that the experiments to be committed will be as much informative as possible for the identification of parameters. The minimization of the information entropy is sought in this step, which, based on asymptotic approximations, depends on the differentiation of the quantities to be measured with respect to the parameters to be identified. The second step is the quantification of the uncertainties [7, 8, 9, 10, 11] i.e. the identification of the values and covariances of the uncertain parameters based on the experimental measurements. The methodology is based on the Bayesian approach and the posterior distribution of the uncertain parameters is estimated by asymptotic expansion and first and second-order adjoint approaches.

The third and fourth steps include the uncertainty propagation and robust design [12, 13, 14, 15, 16, 17, 18]. The propagation of the uncertainties in the parameters to the uncertainties in the quantity of interest, i.e. the objective function, is based on similar asymptotic approximations and adjoint approaches to estimate the mean value and covariance of the quantity of interest given the experimental measurements. The robust optimization of the shape by minimizing the statistical moments of the objective function is achieved through Taylor or asymptotic expansion that include sensitivity derivatives of higher-than-second-order or through derivative-free Gauss-Hermite quadratures on sparse-grids. Alternatively, the reliability-based optimization produces reliable solutions by minimizing the probability of unacceptable performance using adjoint-based reliability index approaches.

The methodologies are applied to the flow above a flat plate the flow through a backward facing step and the external flow around an airfoil.

2 BAYESIAN FRAMEWORK

Assume that $\underline{\theta} \in R^{N_\theta}$ is the vector of parameters of a CFD model that should be estimated using a set of output measurements available from an experiment. Let $\underline{d} \equiv \underline{d}(\underline{x}) \in R^N$ be the vector of measured data of flow quantities obtained from locations $\underline{x}$ in the domain and $\underline{y}(\underline{\theta};\underline{x}) \in R^N$ be the vector of the values of the same quantities computed from a CFD model that correspond to specific values of the parameter set $\underline{\theta}$. The equation

$$\underline{d} = \underline{y}(\underline{\theta};\underline{x}) + \underline{e} \tag{1}$$

is satisfied, where $\underline{e}$ is the prediction error due to model and measurement error. The prediction error is modeled as a Gaussian vector with zero mean and covariance equal to $\Sigma \in R^{N\times N}$. Applying the Bayesian theorem, the posterior probability density function (PDF) of $\underline{\theta}$, given the measured data $\underline{d}$, which represents the uncertainty in the model parameter values based on the

information contained in the measured data, is given by

$$p(\underline{\theta}|\Sigma,\underline{d},\underline{x}) = c\frac{1}{\left(\sqrt{2\pi}\right)^N\sqrt{det\Sigma}}exp\left[-\frac{N}{2}J(\underline{\theta};\Sigma,\underline{d},\underline{x})\right]\pi(\underline{\theta}) \tag{2}$$

where

$$J(\underline{\theta};\Sigma,\underline{d},\underline{x}) = \frac{1}{N}[\underline{d}-\underline{y}(\underline{\theta};\underline{x})]^T\Sigma^{-1}[\underline{d}-\underline{y}(\underline{\theta};\underline{x})] \tag{3}$$

is the measure of the fit between the measured and computed quantities, $\pi(\underline{\theta})$ is the prior distribution for $\underline{\theta}$, and c is a normalization constant so that $\int p(\underline{\theta}|\Sigma,\underline{d},\underline{x})d\underline{\theta} = 1$

3 OPTIMAL SENSOR LOCATION BASED ON INFORMATION ENTROPY

The information entropy which is a scalar measure of the uncertainty in the estimation of the model parameters $\underline{\theta}$ is given by the expression

$$h(\underline{x};\Sigma,\underline{d}) = -\int \ln p(\underline{\theta}|\Sigma,\underline{d},\underline{x})p(\underline{\theta}|\Sigma,\underline{d},\underline{x})d\underline{\theta} \tag{4}$$

depending on the location $\underline{x}$ the sensors are placed. Based on the asymptotic approach for a large amount of experimental data, the information entropy is expressed as [5]

$$h(\underline{x};\Sigma,\underline{d}) \sim H(\underline{x};\underline{\theta}_0,\Sigma) = \frac{1}{2}N_\theta\ln(2\pi) - \frac{1}{2}\det Q(\underline{x};\underline{\theta}_0,\Sigma) \tag{5}$$

where $\underline{\theta}_0$ are the values of $\underline{\theta}$ that minimize $J(\underline{\theta};\Sigma,\underline{d},\underline{x})$ of $\underline{\theta}$ and $Q(\underline{x};\underline{\theta},\Sigma)$ is the semi-positive definite matrix asymptotically given by

$$Q(\underline{x};\underline{\theta},\Sigma) = \nabla_{\underline{\theta}}\underline{y}(\underline{\theta};\underline{x})^T\Sigma^{-1}\nabla_{\underline{\theta}}\underline{y}(\underline{\theta};\underline{x}) \tag{6}$$

computed at the N locations where the sensors are placed. Also, $\nabla_{\underline{\theta}} = [\partial/\partial\theta_1,...,\partial/\partial\theta_{N_\theta}]$. The sensors should be placed within the flow domain in such a way that the measured data are most informative about the parameters of the CFD model. Since the information entropy is the measure of the amount of useful information contained in the data, the sensors should be located at the places that minimize the information entropy

$$\underline{x}_{best} = \arg\min H(\underline{x};\underline{\theta}_0,\Sigma) \tag{7}$$

Gradient-based or stochastic optimization algorithms may be used to find the location $\underline{x}$ of the sensors that minimizes $h(\underline{x};\underline{\theta}_0,\Sigma)$. Since the optimal values of the parameters $\underline{\theta}_0$ and covariance Σ are not known in the initial stage of designing the experiment, the optimization is based on a chosen set of values for $\underline{\theta}_0$ and Σ which are the nominal ones defined by the model.

4 UNCERTAINTY QUANTIFICATION

The objective of uncertainty quantification is to quantify the uncertainty in the parameters $\underline{\theta}^p$ and model the missing (incomplete) information provided by the selected flow model given the experimental data. Probability density functions (PDF) are used to quantify uncertainties and the calculus of probability is employed for handling uncertainties through the model in a consistent manner.

Using a well-established analytical approximation, valid for large number of experimental data, the posterior distribution of the model parameters can be approximated by a multi-variable Gaussian distribution

$$p(\underline{\theta}|\underline{d}) \sim p_a(\underline{\theta}|\underline{d}) = \frac{1}{(2\pi)^{\frac{N_\theta}{2}} detH^{-\frac{1}{2}}} exp\left[-\frac{1}{2}\left(\underline{\theta}-\underline{\hat{\theta}}\right)^T H(\underline{\hat{\theta}})\left(\underline{\theta}-\underline{\hat{\theta}}\right)\right] \tag{8}$$

centered at the most probable value $\underline{\hat{\theta}}$ of the posterior distribution function or equivalently the minimum of the function

$$L(\underline{\theta}) = -log(p(\underline{d}|\underline{\theta})\pi(\underline{\theta})) \tag{9}$$

given by

$$\underline{\hat{\theta}} = \arg\min_{\underline{\theta}} \left[L(\underline{\theta})\right] \tag{10}$$

and with covariance $C(\underline{\hat{\theta}})$ equal to the inverse of the Hessian $H(\underline{\hat{\theta}})$ of the function $L(\underline{\theta})$ estimated at the most probable value $\underline{\hat{\theta}}$. The uncertainty in $\underline{\theta}$ can thus be fully described asymptotically by solving an optimization problem for finding the most probable value $\underline{\hat{\theta}}$ that minimizes the function $L(\underline{\theta})$, and also evaluating the Hessian of the function $L(\underline{\theta})$ at a single point $\underline{\hat{\theta}}$.

5 UNCERTAINTY PROPAGATION

The computation of the mean value and standard deviation of the quantity of interest is based on the asymptotic expansion of the moment integrals using Laplace integration. The idea is to expand the objective function around the value of c that minimizes the minus logarithm of the integrand of each moment.

The mean value of F is computed by the expression

$$\mu_F = (2\pi)^{N/2} F(c^*) p(c^*) |H(c^*)|^{-1/2} \tag{11}$$

where N is the number of uncertain parameters, c^* is the vector of uncertain parameters that minimizes the function $-\ln[F(c)p(c)]$ and $H(c^*)$ is the Hessian matrix of the same function with respect to c computed at c^*.

In the same manner, the standard deviation of the objective function is computed by

$$\sigma_F = \sqrt{\mu_{2,F} - \mu_F^2} \tag{12}$$

where

$$\mu_{2,F} = (2\pi)^{N/2} F^2(c^{**}) p(c^{**}) |H(c^{**})|^{-1/2} \tag{13}$$

where c^{**} is the vector of uncertain parameters that minimizes the function $-\ln[F^2(c)p(c)]$ and $H(c^{**})$ is its Hessian matrix computed at c^{**}.

6 ROBUST OPTIMIZATION

The robust optimization, i.e. the minimization of the mean value and standard deviation of the quantity of interest is based on a gradient or Hessian based descent approach based on their

sensitivities with respect to the design parameters. The first-order derivatives of μ_F with respect to b_k are given by

$$\begin{aligned}\frac{d\mu_F}{db_k} &= (2\pi)^{N/2}\frac{dF(c^*)}{db_k}p(c^*)|H(c^*)|^{-1/2} \\ &- \frac{1}{2}(2\pi)^{N/2}F(c^*)p(c^*)|H(c^*)|^{-3/2}\frac{d|H(c^*)|}{db_k}\end{aligned} \tag{14}$$

while those of σ_F are given by

$$\frac{d\sigma_F}{db_k} = \frac{1}{\sigma_F}\left(\frac{1}{2}\frac{d\mu_{2,F}}{db_k} - \mu_F\frac{d\mu_F}{db_k}\right) \tag{15}$$

where

$$\begin{aligned}\frac{d\mu_{2,F}}{db_k} &= (2\pi)^{N/2}2F(c^{**})\frac{dF(c^{**})}{db_k}p(c^{**})|H(c^{**})|^{-1/2} \\ &- \frac{1}{2}(2\pi)^{N/2}F^2(c^{**})p(c^{**})|H(c^{**})|^{-3/2}\frac{d|H(c^{**})|}{db_k}\end{aligned} \tag{16}$$

where Correspondingly, the second-order sensitivities of μ_F and σ_F with respect to the design parameters are given by

$$\begin{aligned}\frac{d^2\mu_F}{db_k db_l} &= (2\pi)^{N/2}\frac{d^2F(c^*)}{db_k db_l}p(c^*)|H(c^*)|^{-1/2} \\ &- \frac{1}{2}(2\pi)^{N/2}\frac{dF(c^*)}{db_k}p(c^*)|H(c^*)|^{-3/2}\frac{d|H(c^*)|}{db_l} \\ &- \frac{1}{2}(2\pi)^{N/2}\frac{dF(c^*)}{db_l}p(c^*)|H(c^*)|^{-3/2}\frac{d|H(c^*)|}{db_k} \\ &+ \frac{3}{4}(2\pi)^{N/2}F(c^*)p(c^*)|H(c^*)|^{-5/2}\frac{d|H(c^*)|}{db_k}\frac{d|H(c^*)|}{db_l} \\ &- \frac{1}{2}(2\pi)^{N/2}F(c^*)p(c^*)|H(c^*)|^{-3/2}\frac{d^2|H(c^*)|}{db_k db_l}\end{aligned} \tag{17}$$

and

$$\frac{d^2\sigma_F}{db_k db_l} = \frac{1}{\sigma_F}\left(\frac{1}{2}\frac{d^2\mu_{2,F}}{db_k db_l} - \frac{d\mu_F}{db_k}\frac{d\mu_F}{db_l} - \mu_F\frac{d^2\mu_F}{db_k db_l} - \frac{d\sigma_F}{db_k}\frac{d\sigma_F}{db_l}\right) \tag{18}$$

where

$$\begin{aligned}\frac{d^2\mu_{2,F}}{db_k db_l} &= (2\pi)^{N/2}2\left(F(c^{**})\frac{d^2F(c^{**})}{db_k db_l} + \frac{dF(c^{**})}{db_k}\frac{dF(c^{**})}{db_l}\right)p(c^{**})|H(c^{**})|^{-1/2} \\ &- \frac{1}{2}(2\pi)^{N/2}2F(c^{**})\frac{dF(c^{**})}{db_k}p(c^{**})|H(c^{**})|^{-3/2}\frac{d|H(c^{**})|}{db_l} \\ &- \frac{1}{2}(2\pi)^{N/2}2F(c^{**})\frac{dF(c^{**})}{db_l}p(c^{**})|H(c^{**})|^{-3/2}\frac{d|H(c^{**})|}{db_k} \\ &+ \frac{3}{4}(2\pi)^{N/2}F^2(c^{**})p(c^{**})|H(c^{**})|^{-5/2}\frac{d|H(c^{**})|}{db_k}\frac{d|H(c^{**})|}{db_l} \\ &- \frac{1}{2}(2\pi)^{N/2}F^2(c^{**})p(c^{**})|H(c^{**})|^{-3/2}\frac{d^2|H(c^{**})|}{db_k db_l}\end{aligned} \tag{19}$$

The computation of the mean value and standard deviation of the objective function incorporates two optimization problems and the computation of the second-order sensitivities of the objective function with respect to the uncertain variables at each optimal solution.

7 APPLICATIONS

The proposed algorithm for optimal sensor location and uncertainty quantification in CFD is applied to the flow through a 2D backward facing step configuration [19]. The Reynolds number based on step height is equal to 36000 and the inlet Mach number is equal to 0.128. The step height is equal to 1 when the distance of the two walls is equal to 9. A schematic view of the case is shown in Fig. 1.

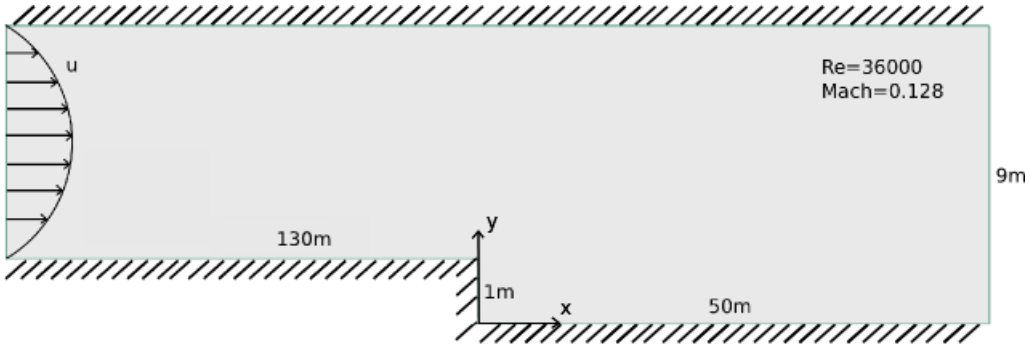

Figure 1: Schematic view of the backward facing step case.

Experimental data for the velocity and Reynolds stress profiles at several axial positions as well as the pressure and friction coefficients at the walls can be found in [19] and are summarized in the $http://turbmodels.larc.nasa.gov/backstep\_val.html$. Herein, the optimal location of profiles of velocities and Reynolds stresses are sought, so that the quantities to be measured will lead to the least uncertainty in the estimates of the model parameters. The area in which the optimal locations of the sensors are sought is the orthogonal area formed a 10×2 rectangular with a height of $2m$ when the step size is equal to $1m$ and a length of $10m$, within which the flow is separated and reattached.

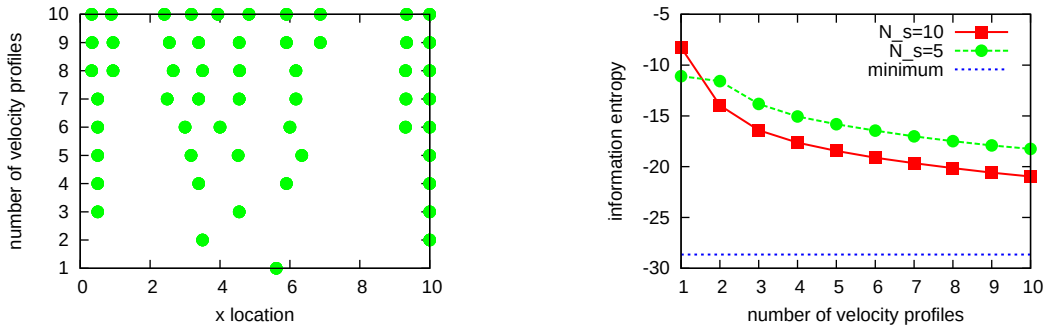

Figure 2: Optimal location of one to ten velocity profiles of five sensors (left) and corresponding information entropy values (right), compared to the minimum possible information entropy.

The design variable vector is defined as $\underline{\delta} = \underline{x} = (x_1, x_2, \ldots, x_p)$ where x_i are the positions of profiles of sensors while the positions of the sensors within each profile are predefined. The number of design variables N_d is equal to the number of profiles N_p. In the cases that follow each profile contains 5 sensors with predefined distances between them. Their positions are $\underline{y} = (0.2, 0.5, 1.0, 1.5, 2.0)$.

Indicative results of optimal locations of one to ten velocity profiles and the corresponding information entropy values are shown in Fig. 2, comparing also to the case that the profile has ten predefined sensors instead of five and to the minimum possible information entropy,

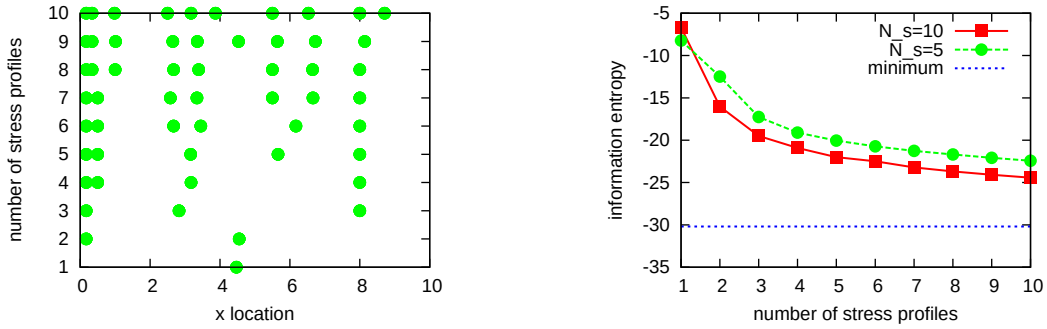

Figure 3: Optimal location of one to ten Reynolds stress profiles of five sensors (left) and corresponding information entropy values (right), compared to the minimum possible information entropy.

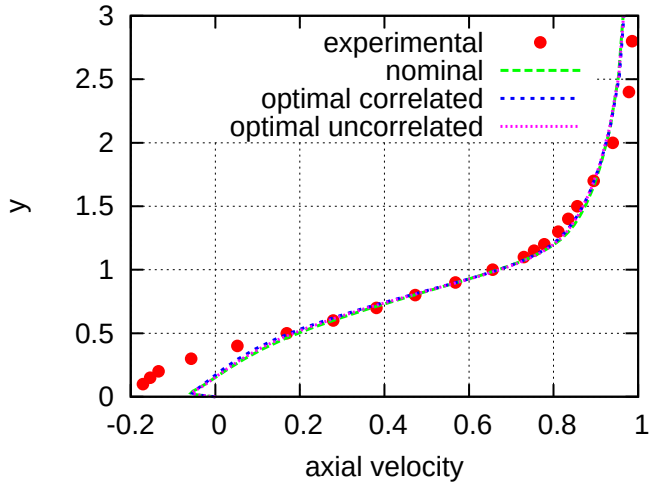

Figure 4: Comparison of the optimal velocity distributions at location $4m$ after the step with experimental measurements.

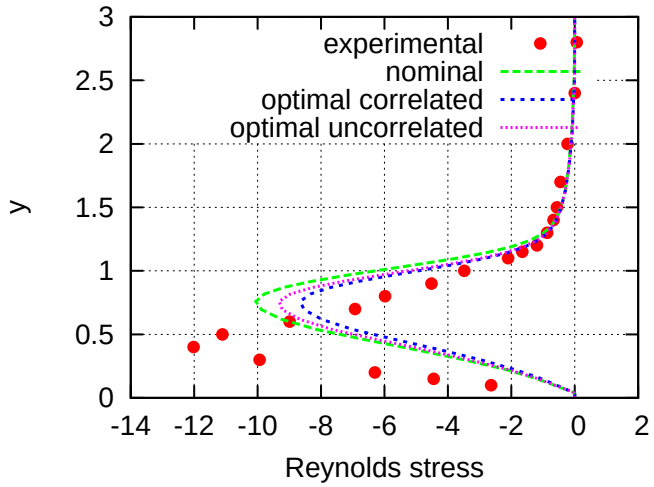

Figure 5: Comparison of the optimal Reynolds stress distributions at location $4m$ after the step with experimental measurements.

obtained in this case by placing a huge number of sensors 60 profiles with 60 sensors with equal distances between them. The information entropy (Fig. 2, right) decreases as the number of

	κ	c_{v1}	c_{v2}	c_{b1}	c_{b2}	c_{w2}
nominal value	0.410	7.100	5.000	0.1355	0.622	0.300
optimal value (correlated)	0.471	6.817	4.950	0.1039	0.639	0.314
optimal value (uncorrelated)	0.456	7.591	4.749	0.1102	0.637	0.335
COV (prior)	0.200	0.200	0.200	0.2000	0.200	0.200
COV (posterior, correlated)	0.109	0.126	0.195	0.0712	0.193	0.172
COV (posterior, uncorrelated)	0.087	0.097	0.200	0.0535	0.194	0.175

Table 1: Initial and optimal parameter values and coefficients of variation (COV) using the adjoint approach for the correlated and the uncorrelated case (first six parameters).

	c_{w3}	σ_{SA}	σ_{VEL}	λ_{VEL}	σ_{RS}	λ_{RS}
nominal value	2.000	0.667	0.035	0.800	1.000	0.200
optimal value (correlated)	1.976	0.770	0.036	0.819	1.156	0.248
optimal value (uncorrelated)	2.074	0.915	0.039	-	1.436	-
COV (prior)	0.200	0.200	-	-	-	-
COV (posterior, correlated)	0.200	0.148	0.145	0.386	0.073	0.189
COV (posterior, uncorrelated)	0.178	0.120	0.062	-	0.064	-

Table 2: Initial and optimal parameter values and coefficients of variation (COV) using the adjoint approach for the correlated and the uncorrelated case (rest six parameters).

sensors increase while the rate of decrease is decreasing. In Fig. 3, the optimal location of one to ten Reynolds stress profiles is shown. The information entropy is decreasing quite a lot upon the placement of the second and third profile and the decrease rate is quite constant from the fourth to the tenth profile.

The quantification of the uncertainties of the eight parameters of the Spalart-Allmaras turbulence model and the parameters of the prediction error model in the flow through the 2D backward facing step configuration follows. In Figs. 4 and 5 the optimal velocity and Reynolds stress distributions at a location $4m$ after the step are compared with experimental measurements.

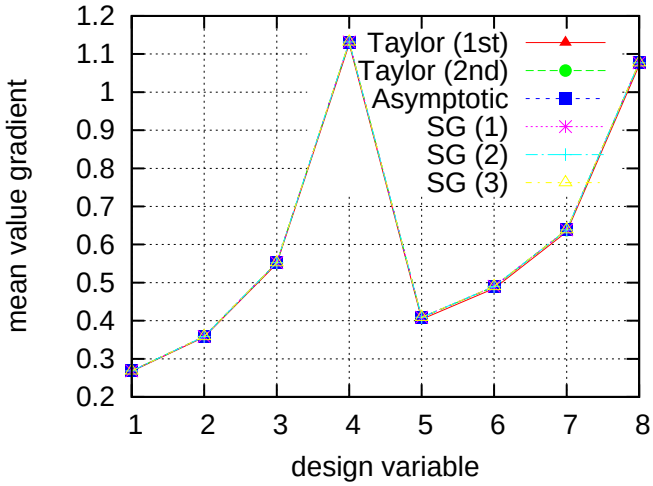

Figure 6: Sensitivity study: Values of the gradient of the mean value of the objective function with respect to the eight shape controlling design variables.

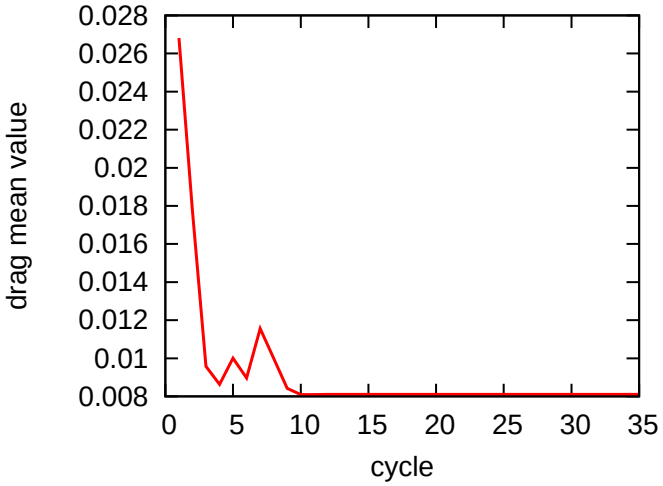

Figure 7: Robust optimization: Minimization of the mean value of drag to lift coefficient. Convergence history of the mean value of the objective function.

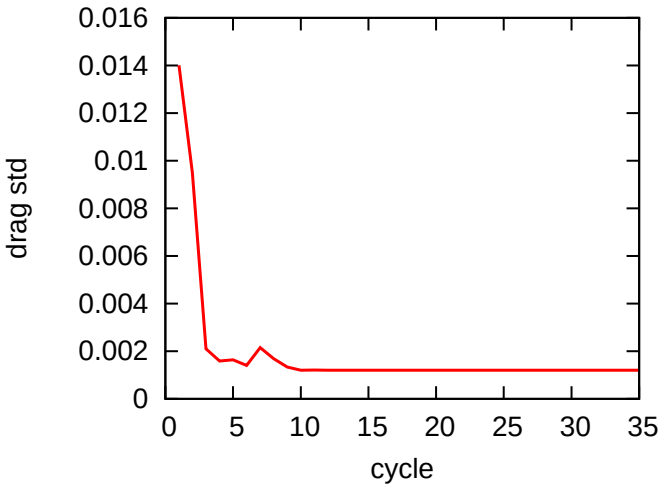

Figure 8: Robust optimization: Minimization of the mean value of drag to lift coefficient. Convergence history of the standard deviation of the objective function.

In Tables 1 and 2, the initial and optimal values of the parameters using the proposed method are shown for correlated and uncorrelated prediction error models. The coefficients of variation (COV) of the marginal distribution of each model parameter, defined as the ratio of the standard deviation over the mean (optimal) value of each model parameter, are also reported in these tables.

Results demonstrate that the measurements provide information for estimating three to five among the eight parameters of the turbulence model, while the rest of the parameters are insensitive to the information contained in the data. Also, it can be seen that the Spalart-Allmaras model is not adequate enough to accurately predict velocities and Reynolds stresses in certain region in the flow domain where flow separation phenomena are dominant.

In the case of uncertainty propagation and robust design, the asymptotic approach is compared in term of computed sensitivities with the Taylor expansion and sparse grid quadrature approaches in the case that the quantity of interest is the lift coefficient of the flow around a 2D airfoil. The first-order sensitivity derivatives of the mean value of the objective function

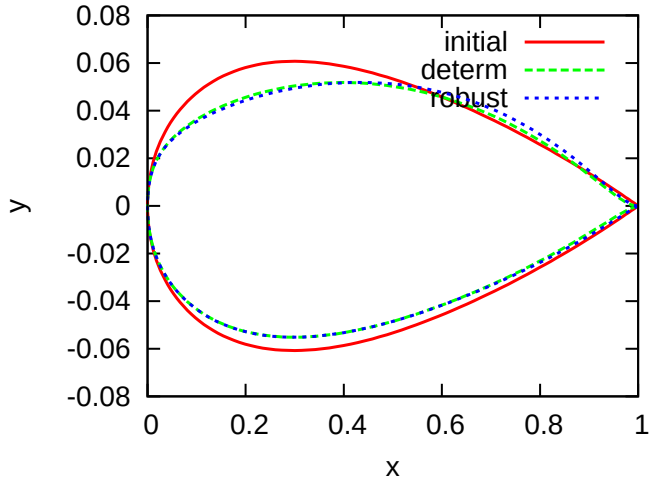

Figure 9: Robust optimization: Comparison of the optimal airfoil contours and the initial one obtained by deterministic and robust optimization.

with respect to the shape controlling parameters are plotted in Fig. 6, comparing the asymptotic expansion with Taylor expansions and grid quadrature approaches. It can be seen that all approaches compute almost equal sensitivity values.

In the case of the robust optimization of the drag to lift ratio, the convergence rates of the mean value and standard deviation of the objective function are shown in figs. 7 and 8. In both deterministic and robust optimization procedures a quasi-Newton algorithm was employed, initialized by the exact Hessian matrix. The latter, in the case of the deterministic example was computed using the most efficient combination of the direct differentiation of the flow equations and the adjoint approach at a cost that scales linearly with the number of design parameters. The optimal airfoil contours for the deterministic and robust optimization cases are shown in fig. 9.

8 Conclusions

The four parts of a posterior robust optimization algorithm based on experimental measurements were presented in this paper. These are the optimal sensor location, uncertainty quantification, uncertainty propagation and robust optimization. The first two were presented in the case of a backward facing step and the rest were validated in the robust aerodynamic optimization of an airfoil. As a future work it is proposed that all four aspects are unified in a single robust optimization procedure, enhanced by optimally conducted experiments.

Acknowledgments

The research project is implemented within the framework of the Action “Supporting Postdoctoral Researchers” of the Operational Program “Education and Lifelong Learning” (Actions Beneficiary: General Secretariat for Research and Technology), and is co-financed by the European Social Fund (ESF) and the Greek State.

REFERENCES

[1] P. Shah, F.E. Udwadia, A methodology for optimal sensor locations for identification of dynamic systems, *Journal of Applied Mechanics*, **45**, 188–196, 1978.

[2] F.E. Udwadia, Methodology for optimal sensor locations for parameter identification in dynamic systems, *Journal of Engineering Mechanics (ASCE)*, **120**(2), 368–390, 1994.

[3] J.E. Alana, Optimal measurement locations for parameter estimation of non linear distributed parameter systems, *Brazilian Journal of Chemical Engineering*, **27**(4), 627–642, 2010.

[4] C. Papadimitriou, J.L. Beck, S.K. Au, Entropy-Based Optimal Sensor Location for Structural Model Updating, *Journal of Vibration and Control*, **6**(5), 781–800, 2000.

[5] C. Papadimitriou, Optimal sensor placement methodology for parametric identification of structural systems, *Journal of Sound and Vibration*, **278**(4), 923–947, 2004.

[6] D.I. Papadimitriou, C. Papadimitriou, Optimal sensor location for model parameter estimation in CFD, 21st AIAA Computational Fluid Dynamics Conference, 24-27 June 2013, San Diego, California.

[7] S.H. Cheung, T.A. Oliver, E.E. Prudencio, S. Prudhomme, R.D. Moser, Bayesian uncertainty analysis with applications to turbulence modeling, *Reliability Engineering and System Safety*, **96**, 1137–1149, 2011.

[8] T.A. Oliver, R.D. Moser, Bayesian uncertainty quantification applied to RANS turbulence models, *Journal of Physics: Conference Series 318*, 2011. doi:10.1088/1742-6596/318/4/042032.

[9] J.E.V. Peter, R.P. Dwight, Numerical sensitivity analysis for aerodynamic optimization: A survey of approaches and applications, *Computers and Fluids*, **39**(3), 373–391, 2011.

[10] D.I. Papadimitriou, C. Papadimitriou, Bayesian estimation of turbulence model parameters using high-order sensitivity analysis, 4th International Congress on Computational Engineering and Sciences (FEMTEC), 19-24 May 2013, Las Vegas.

[11] C. Papadimitriou, D.I. Papadimitriou, Bayesian uncertainty quantification and propagation using adjoint techniques, 5th European Conference on Computational Mechanics (ECCM V), July 20-25, 2014, Barcelona, Spain.

[12] M. Martinelli, R. Duvigneau, On the use of second-order derivatives and metamodel-based Monte-Carlo for uncertainty estimation in aerodynamics, *Computers & Fluids*, **39**(6), 953–964, 2010.

[13] M. Putko, P. Newman, A. Taylor III., L. Green, Approach for uncertainty propagation and robust design in CFD using sensitivity derivatives, AIAA Paper, Vol. 25, No. 28, 2001.

[14] E.M. Papoutsis-Kiachagias, D.I. Papadimitriou, K.C. Giannakoglou, Discrete and continuous adjoint methods in aerodynamic robust design problems, CFD and Optimization, An ECCOMAS Thematic Conference, 2011.

[15] D.I. Papadimitriou, K.C. Giannakoglou, Third-order sensitivity analysis for robust aerodynamic design using continuous adjoint, *International Journal for Numerical Methods in Fluids*, **71**(5), 652–670, 2013.

[16] D.I. Papadimitriou, C. Papadimitriou, Uncertainty propagation for robust aerodynamic shape optimization, 32nd AIAA Applied Aerodynamics Conference, June 2014, Atlanta, Georgia.

[17] D.I. Papadimitriou, C. Papadimitriou, Robust reliability-based aerodynamic shape optimization, 4th International Conference on Engineering Optimization, 8-11 September 2014, Lisbon, Portugal.

[18] D.I. Papadimitriou, C. Papadimitriou, Sensitivity Analysis for Uncertainty Propagation and Robust Design, AIAA Science and Technology Forum and Exposition (SciTech 2015), Kissimmee, Florida, 5-9 January 2015.

[19] D.M. Driver, H.L. Seegmiller, Features of reattaching turbulent shear layer in divergent channel flow, *AIAA Journal*, **23**(2), 163–171, 1985.